A quantum network of clocks

P. Kómár[1†], E. M. Kessler[1,2†], M. Bishof[3], L. Jiang[4], A. S. Sørensen[5], J. Ye[3] and M. D. Lukin[1*]

The development of precise atomic clocks plays an increasingly important role in modern society. Shared timing information constitutes a key resource for navigation with a direct correspondence between timing accuracy and precision in applications such as the Global Positioning System. By combining precision metrology and quantum networks, we propose a quantum, cooperative protocol for operating a network of geographically remote optical atomic clocks. Using nonlocal entangled states, we demonstrate an optimal utilization of global resources, and show that such a network can be operated near the fundamental precision limit set by quantum theory. Furthermore, the internal structure of the network, combined with quantum communication techniques, guarantees security both from internal and external threats. Realization of such a global quantum network of clocks may allow construction of a real-time single international time scale (world clock) with unprecedented stability and accuracy.

With the advances of highly phase coherent lasers, optical atomic clocks containing multiple atoms have demonstrated stability that reaches the standard quantum limit (SQL) set by the available atom number and interrogation time[1–3]. Reaching beyond the SQL, we stand to gain a significant improvement of clock performance by preparing atoms in quantum correlated states (for example, spin squeezed states[4,5]). Here we describe a new approach to maximize the performance of a network composed of multiple clocks, allowing one to gain the advantage of all resources available at each node. Several recent advances in precision metrology and quantum science, along with future improvements in quantum control, may put this approach within reach. On the one hand, phase coherent optical links spanning the entire visible spectrum have been demonstrated, with the capability of delivering the most stable optical oscillator from one colour or location to another[6,7]. On the other hand, quantum communication and entanglement techniques are enabling distant quantum objects to be connected in a quantum network[8–10]. Combining these two technological frontiers, we show here that a distributed network composed of quantum-limited clocks separated by large distances—as appropriate, for example, for satellite-based clocks possibly operated by different nations—can be operated as an ultimate 'world clock', where all members combine their individual resources in a quantum coherent way to achieve greater clock stability and distribute this international time scale in real time for all.

The distributed architecture allows each participant of the network to profit from a stability of the local clock signal that is enhanced by a factor proportional to the total number of parties (as compared to an independent operation of the individual clocks) without losing sovereignty or compromising security. This cooperative gain strongly incentivizes joining the collaborative network while retaining robustness against disruptions of communication channels. On the one hand, the local clocks can be used to identify and correct systematic errors originating from the phase links. On the other hand, the nodes can fall back to relying on the locally stabilized clocks if the phase links fail. We demonstrate that by preparing quantum-correlated states of remote clocks, the network can yield the best possible clock signal allowed by quantum theory for the combined resources. Furthermore, enabled through the use of quantum communication techniques, such a network can be made secure, such that only parties contributing to its operation enjoy the benefit of an ultra-precise clock signal. Besides serving as a real-time clock for the international time scale, the proposed quantum network also represents a large-scale quantum sensor that can be used to probe the fundamental laws of physics, including relativity and connections between space-time and quantum physics.

The concept of a quantum clock network

Figure 1 illustrates the basic concept for the proposed quantum clock network. We consider a set of K atomic clocks (constituting the nodes of the network), each based on a large number of atoms (clock qubits) serving as the frequency reference ω_0 at different geographical locations. In our approach, each clock has its own independently operated local oscillator (LO), $\mathcal{E}_j(t) \propto e^{i\nu_j t}$, with detuning $\delta_j = \nu_j - \omega_0$, $(j = 1, 2, \ldots, K)$. It keeps the time by interrogating its qubits periodically, and uses the measurement data to stabilize the LO frequency at the reference frequency of the atomic transition. However, as opposed to the conventional approach, we consider the situation in which each network node allocates some of its qubits to form entangled states stretching across all nodes. When interrogated within a properly designed measurement scheme, such entangled network states provide ultra-precise information about the deviation of the centre-of-mass (COM) frequency $\nu_{COM} = \sum_j \nu_j / K$ of all local oscillators from the atomic resonance.

Each clock cycle consists of three stages: preparation of the clock atom state (initialization), interrogation by the LOs (measurement) and correction of the laser frequency according to the measurement outcome (feedback). In the further analysis, we assume, for convenience, that in each interrogation cycle one of the nodes plays the role of the centre, which initiates each Ramsey cycle and collects the measurement data from the other nodes via classical channels (Fig. 1b), as well as LO signals via optical links, to feedback the COM signal. (The role of the centre can alternate to provide extra security, see Supplementary Information.) This information, in turn, can be used in a feedback cycle to yield a Heisenberg-limited stability of the COM clock signal generated by the network,

[1]Physics Department, Harvard University, Cambridge, Massachusetts 02138, USA, [2]ITAMP, Harvard-Smithsonian Center for Astrophysics, Cambridge, Massachusetts 02138, USA, [3]JILA, NIST, Department of Physics, University of Colorado, Boulder, Colorado 80309, USA, [4]Department of Applied Physics, Yale University, New Haven, Connecticut 06511, USA, [5]QUANTOP, Danish National Research Foundation Centre of Quantum Optics, Niels Bohr Institute, DK-2100 Copenhagen, Denmark. [†]These authors contributed equally to this work. *e-mail: lukin@physics.harvard.edu
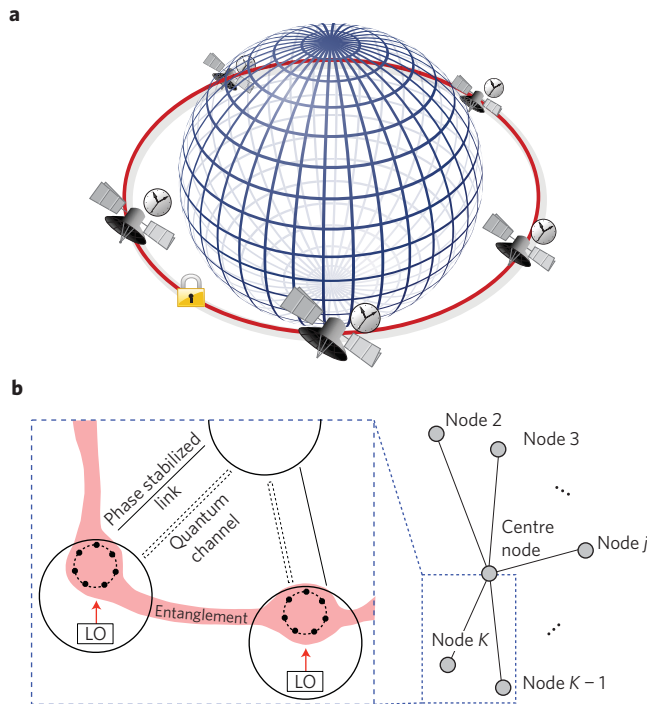
Figure 1 | The concept of world-wide quantum clock network. a, Illustration of a cooperative clock operation protocol in which individual parties (for example, satellite-based atomic clocks from different countries) jointly allocate their respective resources in a global network involving entangled quantum states. This guarantees an optimal use of the global resources, achieving an ultra-precise clock signal limited only by the fundamental bounds of quantum metrology and, in addition, guaranteeing secure distribution of the clock signal. **b**, In addition to locally operating the individual clocks, the different nodes (satellites) employ network-wide entangled states to interrogate their respective local oscillators (LOs). The acquired information is sent to a particular node, serving as a centre, where it is used to stabilize a centre-of-mass mode of the different LOs. This yields an ultra-precise clock signal accessible to all network members.

which is subsequently distributed to the individual nodes in a secure fashion. As a result, after a few cycles, the LOs corresponding to each individual node achieve an accuracy and stability effectively resulting from interrogating atoms in the entire network.

Preparation of network-wide entangled states

In the initialization stage of each clock cycle, entangled states spanning across the nodes at different geographical positions of the network are prepared. In the following, we describe exemplarily how a single network-wide Greenburger–Horne–Zeilinger (GHZ) state can be prepared. The entangled states employed in the proposed quantum network protocol—which is described in the following section—consist of products of GHZ states of different size. They can be prepared by repetition of the protocol that we now describe.

For simplicity, we assume that each node j ($j = 1, \ldots, K$) contains an identical number n of clock qubits, which we label as $1_j, 2_j, \ldots, n_j$ (in the Supplementary Information we discuss the case where the nodes contain different numbers of clock qubits). Further, we assume, for convenience, that the centre node ($j = 1$) has access to an additional $2(K - 1)$ ancilla qubits $a_2, \ldots, a_K, b_2, \ldots, b_K$ besides the n clock atoms (a slightly more complicated procedure allows one to refrain from the use of ancilla qubits, see Supplementary Information). The entangling procedure starts at the centre with the creation of a fully entangled state of one half of the ancilla qubits $\{b_j\}$, and its first clock qubit 1_1. This can be realized, for example, with a single qubit $\pi/2$-rotation (on qubit 1_1)

and a collective entangling operation, which is equivalent to a series of CNOT gates[11] (between 1_1 and each b_j). The result is a GHZ state, $[|00 \ldots 0\rangle_{1_1, b_2, b_3, \ldots, b_K} + i|11 \ldots 1\rangle_{1_1, b_2, b_3, \ldots, b_K}]/\sqrt{2}$. In parallel, the centre uses the other half of the ancillas $\{a_j\}$ to create single Einstein–Podolsky–Rosen (EPR) pairs with each node $j \neq 1$, either by directly sending flying qubits and converting them to stationary qubits, or by using quantum repeater techniques to prepare high-fidelity entanglement[12]. As a result of this procedure, one part of the pair is stored at the centre node (qubit a_j), while the other one is stored at the jth node (qubit 1_j), forming the states $[|00\rangle_{a_j, 1_j} + |11\rangle_{a_j, 1_j}]/\sqrt{2}$ for every j (see Fig. 2).

Next, the centre performs $K - 1$ separate Bell measurements on its ancilla qubit pairs $\{(b_j, a_j)\}$. This teleports the state of qubit b_j to qubit 1_j ($j = 2, \ldots, K$), up to a local single-qubit rotation, which is performed after the measurement outcomes are sent to the node via classical channels. The result of the teleportations is a collective GHZ state $[|00 \ldots 0\rangle_{1_1, 1_2, \ldots, 1_K} + i|11 \ldots 1\rangle_{1_1, 1_2, \ldots, 1_K}]/\sqrt{2}$, stretching across the first qubits of all K nodes.

In the final step of entangling, all nodes (including the centre) extend the entanglement to all of their remaining clock qubits. To do this, each node j performs the collective entangling operation mentioned before based on 1_j and targeting qubits $2_j, 3_j, \ldots, n_j$. At the end of the protocol the different nodes share a common GHZ state $[|\mathbf{0}\rangle + i|\mathbf{1}\rangle]/\sqrt{2}$, where $|\mathbf{0}\rangle$ and $|\mathbf{1}\rangle$ are product states of all qubits $\{i_j : i = 1, 2, \ldots, n, j = 1, 2, \ldots, K\}$ being in $|0\rangle$ or $|1\rangle$, respectively. As discussed below, in practice the entanglement distribution can be done either via polarization- or frequency-entangled photons with frequency difference in the microwave domain, in which case the ancillary qubits involved in the entanglement distribution will be different from the clock qubits. Typically, as part of the preparation process, time delays arise between the initialization of different clock qubits. Its detrimental effects can be entirely avoided by proper local timing or prior preparation of entanglement, as discussed in the Supplementary Information.

Interrogation

The use of entangled resources during the interrogation phase enables an optimal use of the available resources via the following procedure. Assume we have a total of $\tilde{N}$ qubits at our disposal which are equally distributed between the K nodes (indexed $j = 1, \ldots, K$) and prepared in a nonlocal GHZ state $[|\mathbf{0}\rangle + i|\mathbf{1}\rangle]/\sqrt{2}$, where $|\mathbf{0} (\mathbf{1})\rangle \equiv |0(1)\rangle^{\otimes \tilde{N}}$. During the interrogation time T, a clock qubit at node j picks up a relative phase $\phi_j = \delta_j T$. Owing to the non-local character of the state, these phases accumulate in the total state of the atoms $[|\mathbf{0}\rangle + ie^{i\Phi}|\mathbf{1}\rangle]/\sqrt{2}$, where the collective phase after the interrogation time T is given as

$$\Phi = \sum_{j=1}^{K} \frac{\tilde{N}}{K} \phi_j = \tilde{N} \delta_{\mathrm{COM}} T \quad (1)$$

where $\delta_{\mathrm{COM}} = \nu_{\mathrm{COM}} - \omega_0$. To extract the phase information picked up by the different GHZ states, the individual nodes j measure their respective qubits in the x-basis, and evaluate the parity of all measurement outcomes p_j. Subsequently, the nodes send this information to the centre node via a classical channel, where the total parity $p = \prod_j p_j$ is evaluated, and the phase information is extracted[13,14]. Note, that only the full set $\{p_j | j = 1 \ldots K\}$ contains information.

The proportionality with $\tilde{N}$ in equation (1) represents the quantum enhancement in the estimation of δ_{COM}. However, for realistic laser noise spectra, this suggested enhancement is corrupted by the increase of uncontrolled phase slips for a single GHZ state[15]: whenever, after the Ramsey time T, the phase Φ—which owing to the laser frequency fluctuations constitutes a random variable itself—falls out of the interval $[-\pi, \pi]$ the estimation fails. This limitation restricts the maximal Ramsey time to values
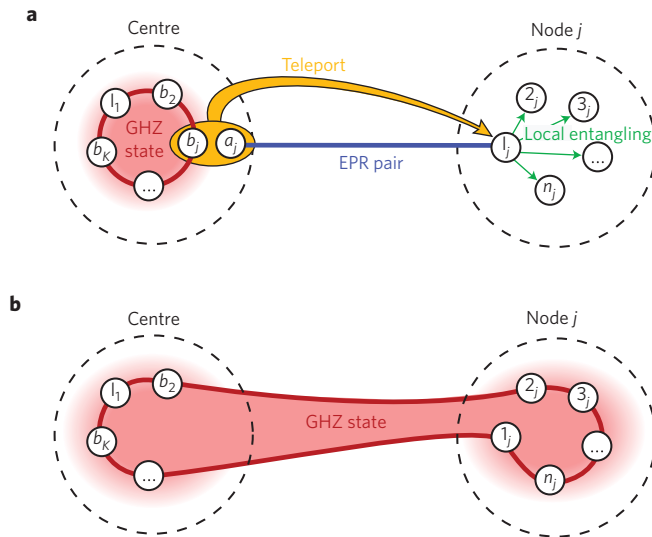
Figure 2 | Entangled state preparation between distant nodes. a, The centre node ($j=1$) initiates the initialization sequence by preparing a local GHZ state across the qubits $\{b_j\}_{j=2}^K$ and 1_1, as well as ($K-1$) EPR pairs on the qubit pairs $\{(a_j, 1_j)\}_{j=2}^K$. Quantum teleportation expands this GHZ state to the first qubit within each of the individual nodes. **b,** Originating from the teleported qubits, the nodes grow the GHZ state to involve all the desired local qubits by employing local entangling operations. The procedure results in common GHZ states over all atoms of the nodes.

$T < (\tilde{N}\gamma_{LO})^{-1}$, where γ_{LO} is the LO linewidth, preventing any quantum gain in the estimation.

To circumvent this problem, we use entangled states consisting of products of successively larger GHZ ensembles, see Supplementary Information and ref. 16. In this approach, atoms are split into several independent, shared groups. We write the number of the first group of atoms as $\tilde{N} = 2^{M-1}K$, for some natural number M. Furthermore, the network shares additional groups of atoms, each containing $2^j K$ ($j = 0, \ldots, M-2$) equally distributed between the nodes and prepared in GHZ states. Moreover, each node has a small number of uncorrelated atoms interrogated by the LOs. Using a protocol reminiscent of the phase estimation algorithm[11,16,17], measurement results from each level j allow one to directly assess the bits $Z_j \in \{0, 1\}$ of the binary fraction representation of the laser phase $\Phi_{LO} = \delta_{COM} T = 2\pi[(Z_1 - 1)2^{-1} + Z_2 2^{-2} + Z_3 2^{-3} \ldots]$ (see Supplementary Section I.B for details). This yields an estimate of Φ_{LO} with Heisenberg-limited accuracy, up to a logarithmic correction, see Supplementary Information:

$$\Delta\Phi_{LO} = \frac{8}{\pi}\log(N)/N \quad (2)$$

even for Ramsey times beyond the limits of the laser frequency fluctuations $[T > (\tilde{N}\gamma_{LO}^{-1})]$, where N represent the total number of clock atoms employed in the scheme. The logarithmic correction arises as a result of the number of particles required to realize this (incoherent) version of the phase estimation algorithm.

Feedback

The measured value of the phase Φ_{LO}, gives an estimate on the COM detuning $\tilde{\delta}_{COM}$ after each Ramsey cycle, which is subsequently used by the centre node to stabilize the COM laser signal. To this end, the centre generates the COM of the frequencies. Every node sends its local oscillator field $\mathcal{E}_i$ to the centre via phase-stable optical links, and the centre synthesizes the COM frequency ν_{COM} by averaging the ν_j frequencies with equal weights. This can be implemented via the heterodyne beat of the local oscillator in the centre against each

incoming laser signal, resulting in K beat frequencies. Synthesizing these beat frequencies allows the local oscillator of the central node to phase track ν_{COM}. The centre distributes the stabilized clock signal to different members of the network by sending individual error signals $\tilde{\delta}_j = \tilde{\delta}_{COM} + (\nu_j - \nu_{COM})$ to all nodes j, respectively, and corrects its own LO as well, accordingly. Alternatively, the centre can be operated to provide restricted feedback information to the nodes (Supplementary Information).

Stability analysis

In this section, we demonstrate that the proposed quantum clock network achieves the best clock signal allowed by quantum theory for the available resources, that is the total atom number. To quantify this cooperative gain, we compare networks of different types (classical or quantum mechanical interrogation of the respective LOs) and degrees of cooperation (no cooperation, classical, or quantum cooperation).

First, we analyse the stability of the proposed quantum clock network, corresponding to the case of quantum interrogation and cooperation curve (a) in Fig. 3. In this case, the analysis resulting in equation (2) suggests that near-Heisenberg-limited scaling with a total atom number can be achieved for the entangled clock network. In particular, for a given total particle number N and for averaging times shorter than the timescale set by individual qubit noise $\tau < 1/(\gamma_i N)$ (where γ_i is the atomic linewidth, the factor N results from the enhanced decoherence of the entangled interrogation state[18]), the network operation achieves a Heisenberg-limited Allan deviation (ADEV) of the COM laser mode

$$\sigma_y(\tau) \sim \frac{\sqrt{\log(N)}}{\omega_0 N} \frac{1}{\tau} \quad (3)$$

up to small numerical corrections (see Supplementary Information). The $1/\tau$ scaling results from the effective cancellation of the low-frequency part of the laser noise spectrum, achieved by the cascaded protocol described above, possibly in combination with additional stages of uncorrelated interrogations using varying Ramsey times[19,20]; see ref. 16. This allows the cycle time T (which is assumed to be equal to the interrogation time) to be extended to the total available measurement time τ.

Eventually, for large averaging times $\tau > 1/(\gamma_i N)$ the Ramsey time becomes fundamentally limited by individual noise processes that determine the atomic linewidth $T \leq 1/(\gamma_i N)$. As a result, the $1/N$ scaling breaks down, and the ADEV returns to the square root scaling with both the employed particle number and averaging time,

$$\sigma_y(\tau) \sim \frac{1}{\omega_0 \sqrt{N}} \sqrt{\frac{\gamma_i}{\tau}} \quad (4)$$

up to constant numerical factors. Equation (4) results from fundamental quantum metrological bounds[21] (in the case of dominating trap losses, the loss rate simply replaces γ_i in the above formula), and represents the best conceivable clock stability in the presence of individual particle decoherence which, in a network, can only be achieved via cooperation. Independently operating a clock, in contrast, can only achieve a stability scaling with the local number of atoms (that is, $\sigma_y(\tau) \propto \sqrt{K/N}$).

Figure 3 illustrates the comparison of an entangled clock network with other approaches. A network in which the K nodes cooperate classically (curve (b)), by locally measuring the individual phase deviation ϕ_j, and combining the outcomes via classical channels, outperforms individually operated clocks (curve (c)) by a factor of $\sqrt{K}$ (for both cases, assuming optimal quantum interrogation for individual nodes[16,22]). The quantum network protocol (curve (a)) increases this cooperative advantage by an additional factor of $\sqrt{K}$ for short averaging times, while the ADEV converges to the
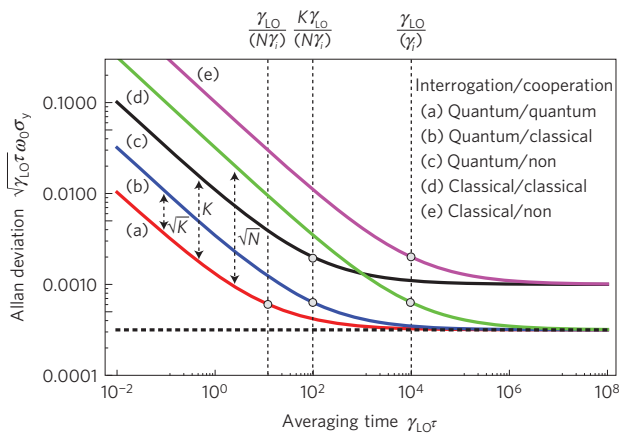
Figure 3 | Performance of different operation schemes. Comparison of the achievable (rescaled) Allan deviation $\sqrt{\gamma_{LO}\tau}\omega_0\sigma_y$ using clock networks of different types and degrees of cooperation. **a**, The proposed protocol realizing quantum interrogation and cooperation (red). **b**, Quantum interrogation and classical cooperation (blue). **c**, Quantum interrogation and no cooperation (black). **d**, Classical interrogation and classical cooperation (green). **e**, Classical interrogation and no cooperation (violet; see text). The dotted base line represents the fundamental bound arising from the finite width of the clock atoms transition (compare equation (4)). This optimal stability can be attained only by cooperation between the nodes. The fully quantum clock network (**a**) represents the optimal form of cooperation, and reaches this boundary faster than any other operational mode. Parameters are $N = 1{,}000$, $K = 10$, $\gamma_i = 10^{-4}\gamma_{LO}$.

fundamental bound of equation (4) K times faster compared to the case of classical cooperation (curve (b)). Although an optimal, classical protocol (for example, refs 19,20), combined with classical cooperation (curve (d)), eventually reaches the same stability, this approach is atom-shot-noise limited, and hence its performance is reduced by a factor of $\sqrt{N}$ for short averaging times compared to the quantum network protocol. Consequently, the optimal stability (equation (4)) is reached at averaging times that are N times longer than for the proposed quantum network. Naturally, all of the above approaches are superior to a classical scheme without cooperation (curve (e)).

As a specific example, we first consider ion clocks that can currently achieve a stability of 2.8×10^{-15} after 1 s of averaging time[23]. The entangled states of up to 14 ions has already been demonstrated[24], as was the entanglement of remote ions[25]. We consider a network of ten clocks, each containing ten ions. Using Al$^+$ ($\omega_0 = 2\pi \times 1121$ THz, $\gamma_i = 2\pi \times 8$ mHz), we find that the quantum cooperative protocol can reach 4×10^{-17} fractional frequency uncertainty after 1 s. Larger improvements could potentially be achieved by using, for example, Yb$^+$ ions, owing to the long coherence time (2.2×10^4 s) of its octupole clock transition.

The quantum gain could be even more pronounced for neutral atomic clocks. For a network consisting of ten clocks similar to the one operated in JILA (ref. 1), each containing 1,000 neutral atoms with central frequency $\omega_0 = 2\pi \times 429$ THz and linewidth $\gamma_i = 2\pi \times 1$ mHz, the quantum cooperative scheme can achieve a stability of $\sim 2 \times 10^{-18}$ after 1 s averaging, and is an order of magnitude better than the best classical cooperative scheme. Future advances, employing clock transitions with linewidths of a few tens of µHz (such as erbium), could possibly allow for further improvement, achieving fractional frequency uncertainty beyond 10^{-20} after $\tau \sim 100$ s. This level of stability is of the same order of magnitude as the required sensitivity to successfully use the network as a gravitational interferometer[26].

So far we have assumed perfect operation and infinitely fast entanglement distribution rates. In the Supplementary Information
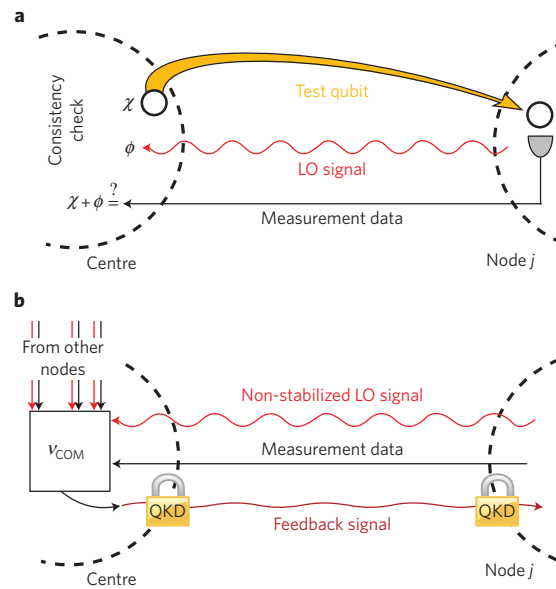

Figure 4 | Schematics of security countermeasures. a, The centre node can choose to test any node j by teleporting a disentangled qubit with a certain phase rotation. A properly operating node creates a local GHZ state $[|0\rangle + e^{i\chi}|1\rangle]/\sqrt{2}$ from the sent qubit, measures the parity of the GHZ state, and sends the result to the centre. The measured parity holds information on the phase $\phi' = \chi + \phi$, where ϕ is the accumulated phase of the local oscillator (LO) at the node. The centre verifies ϕ by comparing it with the classically determined phase of the sent LO signal with respect to the centre-of-mass signal. **b**, Eavesdropping can be prevented by prescribing that only the non-stabilized LO signals are sent through classical channels and encoding the radio frequency feedback signal with phase modulation according to a shared secret key.

we analyse these assumption and find that the advantage of our scheme persists provided that fidelity of the local collective entangling[27] (which creates a GHZ state of N/K qubits) exceeds the threshold fidelity F_{th}, where $1 - F_{th} \sim 1/(K\log N)$, and the EPR sharing rate is higher than $R_{EPR} \sim (\log N)^2\gamma_i$. For the optical clock example presented above, $F_{th} \sim 0.99$, and $R_{EPR} \sim 1$ Hz. Although local operations with fidelity ~ 0.95 have been realized for $N \sim 5$ ions[24], the errors in such operations increase with N, making this realization more challenging.

Security

A network with such precise time-keeping capabilities can be subject to both internal and external attacks. Effectively countering them is crucial to establish a reliable ground for cooperation. We consider the network secure if the implemented countermeasures can prevent external parties from benefiting from the network (eavesdropping), as well as effectively detect any malicious activities of any of the members (sabotage).

Sabotage describes the situation where one of the nodes—intended or unintended—operates in a damaging manner. For example, one node could try sending false LO frequencies or wrong measurement bits in the hope of corrupting the collective measurement outcomes. To detect such malicious participants, the central node can occasionally perform assessment tests of the different nodes by teleporting an uncorrelated qubit state $[|0\rangle + e^{i\chi}|1\rangle]/\sqrt{2}$, where χ is a randomly chosen phase known only to the centre. By checking for statistical discrepancies between the measurement results and the detuning of the LO signal sent by the node under scrutiny, the centre can rapidly and reliably determine whether the particular node is operating properly (see Fig. 4a and Supplementary Information), however this strategy breaks down if multiple sabotage attacks happen within a short time.

Eavesdropping, that is, the unauthorized attempt to access the stabilized ν_{COM} frequency, can be prevented by encoding the classical channels, over which the centre and the nodes exchange feedback signals, using quantum key distribution protocols[28]. Our protocol can keep the stabilized signal hidden from outsiders by mixing the feedback signal with the LO signal at each node only after the non-stabilized LO has been sent to the centre (Fig. 4b and Supplementary Information). As a result, even if all LO signals are intercepted, the eavesdropper is able to access only the non-stabilized COM signal. Furthermore, the centre exclusively can decode the measurement results sent by the individual nodes using its own measurement outcomes as mentioned above. As a result, the stabilized COM signal remains accessible exclusively to parties involved in the collaboration.

Finally, we note that a distributed operation offers significant security advantages over an alternative approach of having all resources combined in one place from where the signal is distributed. In case of a physical attack of the network, disabling the centre or the communication links, the nodes can fall back to an independent clock operation using their local resources.

Outlook

One of the advantages of the proposed quantum clock network involves its ability to maintain and synchronize the time standards across multiple parties in real-time. Unlike the current world time standard, where the individual signals from different clocks are averaged and communicated with a time delay (a so-called paper clock), in our quantum clock network all participants have access to the ultra-stable signal at any time. This makes it possible to measure systematic errors of different clocks in real time, which in turn allows one to correct them[1], unlike in the case of the paper clock, which has to rely on the retrospectively averaged time signals (Supplementary Information). The enhanced stability of the network signal hereby allows longer Ramsey times in the control measurements used to determine the systematics of the single clock. Furthermore, by having full access to their local clocks, the different parties keep their full sovereignty and ensure security, as opposed to a joint operation of a single clock.

Realization of the full-scale network of the type described here will require a number of technological advances in both metrology and experimental quantum information science. The remote entanglement can be implemented by using recently demonstrated techniques for individual atom–photon entanglement[29–33]. Because the teleportation protocol requires quantum links capable of sharing EPR pairs with sufficiently high repetition rate and fidelity, entanglement purification[34] and quantum repeater techniques[12] will probably be required. In practice, qubits used for entanglement distribution may not be ideal for clocks. However, as noted previously, remote entanglement does not need to involve coherent qubits at optical frequencies (for example, polarization entanglement can be used). In such a case, the use of hybrid approaches, combining different systems for entanglement and local clock operations, may be warranted. Similarly, signals from clocks employing different transition frequencies can be coherently connected by frequency combs, allowing clocks with different clock qubits to participate. It might also be interesting to explore if high-fidelity entangled EPR pairs can be used to create remote entangled states of spin-squeezed type[4,35,36], or by following the proposed approach for cat state preparation in atomic ensembles[37], or using collective interactions (such as ref. 27) and repetitive teleportation[38]. Furthermore, although space-based communication networks will be capable of maintaining optical phase coherence for the links between clocks, we note that establishing ground-space coherent optical links remains a technical challenge and requires an intense research effort which has recently started[39]. Finally, if the entire network is spanned by satellites in space, the on-board local oscillators can further benefit from the much lower noise level compared to ground-based clocks.

If realized, such a quantum network of clocks can have important scientific, technological and social consequences. Besides creating a world platform for time and frequency metrology, such a network may find important applications in a range of technological advances for earth science[40], precise navigation of autonomous vehicles and space probes (requiring high refresh rate), and in the testing of and search for fundamental laws of nature, including relativity and the connection between quantum and gravitational physics[26,41–43]. To explore these exciting applications one can either use the excellent common frequency reference generated by the clock network, or, alternatively, prepare modified collective states of different nodes that can directly measure the specific signal under study.

References

1. Bloom, B. *et al.* An optical lattice clock with accuracy and stability at the 10^{-18} level. *Nature* **506,** 71–75 (2014).
2. Hinkley, N. *et al.* An atomic clock with 10^{-18} instability. *Science* **341,** 1215–1218 (2013).
3. Nicholson, T. L. *et al.* Comparison of two independent Sr optical clocks with 1×10^{-17} stability at 10^3 s. *Phys. Rev. Lett.* **109,** 230801 (2012).
4. Leroux, I. D., Schleier-Smith, M. H. & Vuletić, V. Implementation of cavity squeezing of a collective atomic spin. *Phys. Rev. Lett.* **104,** 073602 (2010).
5. Buzek, V., Derka, R. & Massar, S. Optimal quantum clocks. *Phys. Rev. Lett.* **82,** 2207–2210 (1999).
6. Ye, J. *et al.* Delivery of high-stability optical and microwave frequency standards over an optical fiber network. *J. Opt. Soc. Am. B* **20,** 1459–1467 (2003).
7. Droste, S. *et al.* Optical-frequency transfer over a single-span 1840 km fiber link. *Phys. Rev. Lett.* **111,** 110801 (2013).
8. Cirac, J., Zoller, P., Kimble, H. & Mabuchi, H. Quantum state transfer and entanglement distribution among distant nodes in a quantum network. *Phys. Rev. Lett.* **78,** 3221–3224 (1997).
9. Kimble, H. J. The quantum internet. *Nature* **453,** 1023–1030 (2008).
10. Perseguers, S., Lapeyre, G. J., Cavalcanti, D., Lewenstein, M. & Acín, A. Distribution of entanglement in large-scale quantum networks. *Rep. Prog. Phys.* **76,** 096001 (2013).
11. Nielsen, M. A. & Chuang, I. L. *Quantum Computation and Quantum Information* (Cambridge Univ. Press, 2000).
12. Duan, L. M., Lukin, M. D., Cirac, J. I. & Zoller, P. Long-distance quantum communication with atomic ensembles and linear optics. *Nature* **414,** 413–418 (2001).
13. Bollinger, J., Itano, W., Wineland, D. & Heinzen, D. Optimal frequency measurements with maximally correlated states. *Phys. Rev. A* **54,** R4649–R4652 (1996).
14. Leibfried, D. *et al.* Toward Heisenberg-limited spectroscopy with multiparticle entangled states. *Science* **304,** 1476–1478 (2004).
15. Wineland, D. *et al.* Experimental issues in coherent quantum-state manipulation of trapped atomic ions. *J. Res. Natl Inst. Stand. Technol.* **103,** 259–328 (1998).
16. Kessler, E. M. *et al.* Heisenberg-limited atom clocks based on entangled qubits. *Phys. Rev. Lett.* **112,** 190403 (2014).
17. Giedke, G., Taylor, J., D Alessandro, D., Lukin, M. & Imamolu, A. Quantum measurement of a mesoscopic spin ensemble. *Phys. Rev. A* **74,** 032316 (2006).
18. Huelga, S. F. *et al.* Improvement of frequency standards with quantum entanglement. *Phys. Rev. Lett.* **79,** 3865–3868 (1997).
19. Rosenband, T. & Leibrandt, D. R. Exponential scaling of clock stability with atom number. Preprint at http://arXiv.org/abs/1303.6357 (2013).
20. Borregaard, J. & Sørensen, A. S. Efficient atomic clocks operated with several atomic ensembles. *Phys. Rev. Lett.* **111,** 090802 (2013).
21. Escher, B. M., de Matos Filho, R. L. & Davidovich, L. General framework for estimating the ultimate precision limit in noisy quantum-enhanced metrology. *Nature Phys.* **7,** 406–411 (2011).
22. Borregaard, J. & Sørensen, A. S. Near-Heisenberg-limited atomic clocks in the presence of decoherence. *Phys. Rev. Lett.* **111,** 090801 (2013).
23. Chou, C. W., Hume, D. B., Koelemeij, J. C. J., Wineland, D. J. & Rosenband, T. Frequency comparison of two high-accuracy Al$^+$ optical clocks. *Phys. Rev. Lett.* **104,** 070802 (2010).
24. Monz, T. *et al.* 14-qubit entanglement: Creation and coherence. *Phys. Rev. Lett.* **106,** 130506 (2011).

25. Maunz, P. *et al.* Quantum interference of photon pairs from two remote trapped atomic ions. *Nature Phys.* **3,** 538–541 (2007).
26. Schiller, S. *et al.* Einstein Gravity Explorer—A medium-class fundamental physics mission. *Exp. Astron.* **23,** 573–610 (2008).
27. Sørensen, A. & Mølmer, K. Entanglement and quantum computation with ions in thermal motion. *Phys. Rev. A* **62,** 022311 (2000).
28. Gisin, N., Ribordy, G., Tittel, W. & Zbinden, H. Quantum cryptography. *Rev. Mod. Phys.* **74,** 145–195 (2002).
29. Olmschenk, S. *et al.* Quantum teleportation between distant matter qubits. *Science* **323,** 486–489 (2009).
30. Chou, C-W. *et al.* Functional quantum nodes for entanglement distribution over scalable quantum networks. *Science* **316,** 1316–1320 (2007).
31. Togan, E. *et al.* Quantum entanglement between an optical photon and a solid-state spin qubit. *Nature* **466,** 730–734 (2010).
32. Bernien, H. *et al.* Heralded entanglement between solid-state qubits separated by three metres. *Nature* **497,** 86–90 (2013).
33. Ristè, D. *et al.* Deterministic entanglement of superconducting qubits by parity measurement and feedback. *Nature* **502,** 350–354 (2013).
34. Dür, W., Briegel, H-J., Cirac, J. & Zoller, P. Quantum repeaters based on entanglement purification. *Phys. Rev. A* **59,** 169–181 (1999).
35. Sherson, J. F. *et al.* Quantum teleportation between light and matter. *Nature* **443,** 557–560 (2006).
36. Ma, X-S. *et al.* Quantum teleportation over 143 kilometres using active feed-forward. *Nature* **489,** 269–273 (2012).
37. McConnell, R. *et al.* Generating entangled spin states for quantum metrology by single-photon detection. *Phys. Rev. A* **88,** 063802 (2013).
38. Andersen, U. L. & Ralph, T. C. High fidelity teleportation of continuous variable quantum states using delocalized single photons. *Phys. Rev. Lett.* **111,** 050504 (2013).
39. Djerroud, K. *et al.* Coherent optical link through the turbulent atmosphere. *Opt. Lett.* **35,** 1479–1481 (2010).
40. Tapley, B. *et al.* GGM02—An improved Earth gravity field model from GRACE. *J. Geod.* **79,** 467–478 (2005).
41. Abramovici, A. *et al.* LIGO: The laser interferometer gravitational-wave observatory. *Science* **256,** 325–333 (1992).
42. Seidel, A. *et al.* 2007 IEEE International Frequency Control Symposium Joint with the 21st European Frequency and Time Forum 1295–1298 (IEEE, 2007).
43. Wolf, P. *et al.* Quantum physics exploring gravity in the outer solar system: The SAGAS project. *Exp. Astron.* **23,** 651–687 (2008).

Acknowledgements

Author contributions

All authors contributed extensively to the work presented in this paper.

Additional information

Supplementary information is available in the online version of the paper. Reprints and permissions information is available online at www.nature.com/reprints. Correspondence and requests for materials should be addressed to M.D.L.

Competing financial interests

The authors declare no competing financial interests.